Lithos, 26 (1990) 43–65
Elsevier Science Publishers B.V., Amsterdam

The Bayan Obo iron–rare-earth–niobium deposits, Inner Mongolia, China

Lawrence J. Drew[a], Meng Qingrun[b] and Sun Weijun[b]
[a]*U.S Geological Survey, Reston, Va. (U.S.A.)*
[b]*Tianjin Geologic Research Academy, Tianjin (China)*

(Received January 9, 1990; accepted June 10, 1990)

LITHOS

ABSTRACT

Drew, L.J., Meng, Q. and Sun, W., 1990. The Bayan Obo iron–rare-earth–niobium deposits, Inner Mongolia, China. In: A.R. Woolley and M. Ross (Editors), Alkaline igneous rocks and carbonatites. Lithos, 26: 43–65.

The plate tectonic setting, regional geology and certain aspects of the economic geology of the iron–rare-earth–niobium ore bodies at Bayan Obo, Inner Mongolia, China, were studied by a team of geologists from the Tianjin Geologic Research Academy and the U.S. Geological Survey between 1987 and 1989. These ore bodies were formed by hydrothermal replacement of Middle Proterozoic dolomite in an intracontinental rift setting. A variety of veins and/or dikes that have a carbonatitelike mineralogy cut the footwall clastic rocks and migmatites. A stockwork of veins occurs at several locations in the footwall. The hanging wall is a shale that has been converted to a K-metasomatite and has microcrystalline potassium feldspar as its principal constituent. This shale served as a sealing caprock that contained the chemical solutions that reacted with the dolomite and created the enormous concentration of mineralized rock in an 18-kilometer-long syncline. The rocks that host these ore bodies and the associated mineralized areas occur today as roof pendants in granitoid rocks of Permian age that were emplaced during a continent-to-continent collision during that period.

Introduction

The Bayan Obo iron–rare-earth–niobium ore bodies, which are located in Inner Mongolia, China, at latitude 41.7 degrees north and longitude 110.0 degrees east (Fig. 1), are interpreted as being hydrothermal replacement deposits (Tugarinov, 1963; Vlasov, 1968). They are located in a syncline that extends for 18 km along its axis and is 1 to 3 km wide. More than 20 open pits have been worked since mining began in 1957. The reported total reserves are at least 1500 million metric tons of iron (average grade 35%), at least 48 million tons of rare-earth oxides (average grade 6%) and about 1 million tons of niobium (average grade 0.13%). The two largest open pits, the Main and the East mines, contain more than 60% of the total reserves.

Bayan Obo is 146 km by road north of Baotou (population 1.5 million), where the ores are concentrated and smelted. The climate at Bayan Obo is extremely dry. The surrounding countryside is sparsely vegetated high prairie and has excellent exposures of Archean migmatites, Proterozoic and Paleozoic sedimentary rocks and Paleozoic igneous rocks. About 40,000 people live at Bayan Obo, most of whom work either directly in mining or in support activities.

This paper, which describes the regional geology of the Bayan Obo area, is based on previous investigations reported in the Chinese and the Russian literature and on field studies during July 1987 and September 1988; color composite and stereo satellite imagery were used in these studies. The geologic setting of the ore bodies, the characteristics of as-

0024-4937/90/$03.50

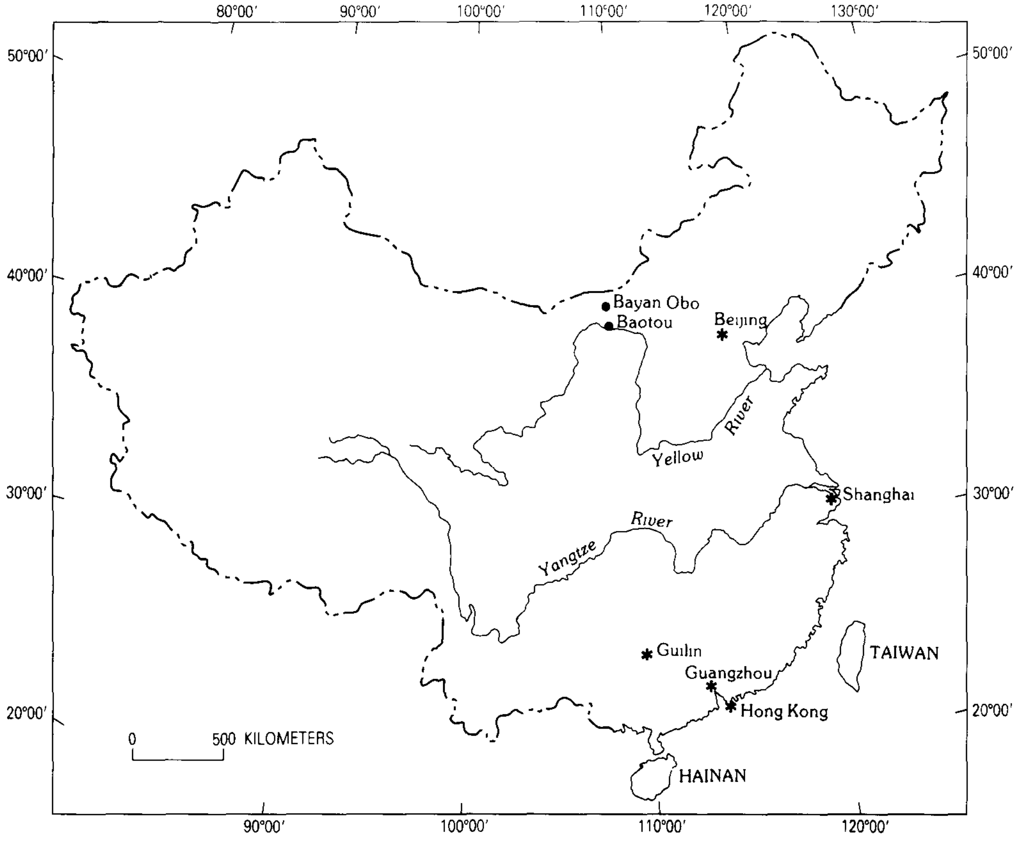

Fig. 1. Map showing location of Bayan Obo.

sociated veins and stockworks and the pervasive alteration of the host rocks are discussed. The origin of these ore bodies is interpreted on the basis of the plate tectonic setting of the north China plate, field relations and the mineralogy and the geochemistry of samples collected in the field. This research was performed under an agreement between the Tianjin Geologic Research Academy of the Ministry of Metallurgical Industry of China and the U.S. Geological Survey signed in Reston, Va., on April 24, 1987.

Stratigraphy and regional geology

The Bayan Obo ore bodies occur as hydrothermal replacements of the dolomite unit (*Y8*) of the Bayan Obo Group of Middle Proterozoic age (Fig. 2; Meng, 1982). The Bayan Obo Group is a series of clastic and carbonate rocks that was deposited in a series of grabens upon an Archean basement of migmatites of the Wu Tai Group. During the Paleozoic, these rocks were intruded by several compositionally distinct granitoid suites; the largest in volume by far were the granites of Permian age. The Bayan Obo Group rocks and Archean migmatites occur today as roof pendants in these granites (Drew and Meng, 1990).

The oldest rocks that crop out in the Bayan Obo area are the Wu Tai migmatites (A_{wt}), the melansomes of which are interpreted to be restites and granites. A large hiatus is believed to exist between the formation of these migmatites at 2350 Ma and the deposition of the basal conglomerate of the Bayan Obo Group (*Y1*) between 1350 and 1650 Ma (Ren et al., 1987). We recognize that in the United States, the Archean–Proterozoic boundary is set at 2500 Ma, whereas, in China, younger rocks, such as the Wu Tai series, are considered to be Archean in age. We also have used the symbol *Y* for rocks of Middle Proterozoic age, which is the map-unit convention in North America. In the Chinese literature, the symbol H is used for these rocks, which probably refers to the word "horizon", a field term

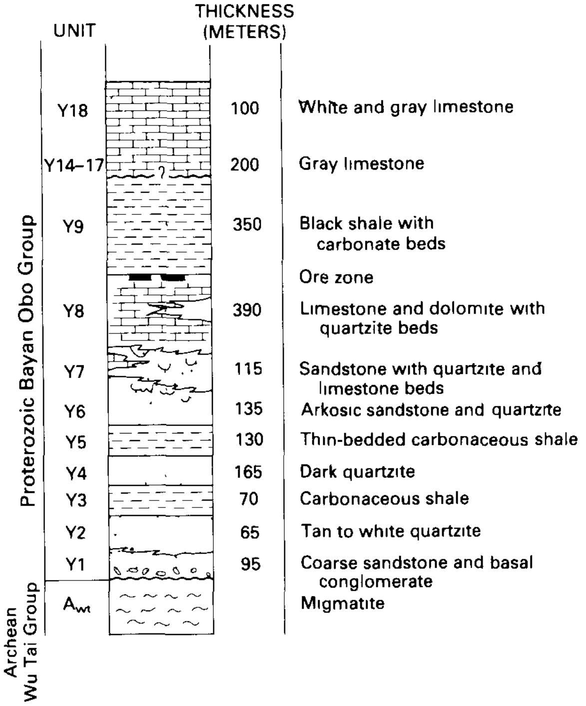

Fig. 2. Archean and Proterozoic stratigraphic section at Bayan Obo (modified from Meng, 1982).

for a rock unit presumably adapted from the earlier Russian literature (Tugarinov, 1963).

The basal conglomerate (*Y1*) of the Bayan Obo Group contains coarse-grained beds, several of which include pebbles larger than 5 cm in diameter. The upper contact of this unit is gradational with the overlying orthoquartzite (*Y2*), which averages 65 m in thickness. The next three units, the shale (*Y3*), the quartzite (*Y4*) and the shale (*Y5*) (Fig. 2), can be mapped easily in the field because of the distinctive doublet of *Y3* and *Y5* shale and the overlying reddish-weathered *Y6* arkosic sandstone. The contacts between the *Y6* arkosic sandstone and the *Y7* sandstone units and between the *Y7* sandstone and the *Y8* carbonate units are transitional. These three units taken together display a transition from coarse-grained basal arkose (regressive pulse of sediment) through repeated transgressive and regressive pulsations during the time of deposition of the upper part of *Y6* and through much of the deposition of the *Y7* unit to the deposition of carbonates in the *Y8* unit.

The *Y8* carbonate unit is, for the most part, a gray limestone that varies in thickness across the Bayan Obo area. In the ore-bearing syncline, this unit is a tan dolomite and also contains thin shale beds and scattered beds of orthoquartzite. The variation in thickness of this unit is assumed to be controlled by local depositional features, such as movement on faults in the graben systems, that were active at the time of deposition.

The base of the *Y8* carbonate unit is characterized by a barrier-island sequence containing numerous tidal channels filled with quartzose material. These channels commonly are from 1 to 3 m across and 0.5 to 1 m deep. Beneath the Main mine, this part of the stratigraphic section has been structurally disrupted by thrust faulting. We believe that much of the confusion over the means of emplacement of the ore bodies at Bayan Obo has resulted from a misinterpretation of field relations observed in outcrops of this basal section of the *Y8* unit (Zhou et al., 1980; Bai and Yuan, 1985). Without paleoenvironmental reconstruction, it would not be unreasonable to interpret the jumble of juxtaposed beds of quartzite and carbonate as evidence that a carbonatitic magma stoped its way into the Bayan Obo Group and that the Main mine ore was directly associated with this magmatic activity. The large amount of sedimentological evidence in outcrops near the main pit, such as bedding structures and ripple marks, along with the fossil evidence (stromatolites, algae and bacteria; Meng, 1982; Hou Zonglin, 1987), points clearly to a sedimentary origin of the carbonate rocks mapped as the *Y8* limestone and dolomite.

The 350-m-thick *Y9* shale was deposited conformably upon the *Y8* carbonate unit. This shale is widely exposed in the Bayan Obo area in various thrust slices, large folds and fault melanges (Fig. 3). The shale appears to have served as a seal to the hydrothermal system that formed the ore bodies at Bayan Obo. In the core of the syncline (hanging wall) that hosts the ore bodies, this shale was extensively altered by K-metasomatism. At other locations in the area, it was metamorphosed in contact aureoles related to Permian granitoid intrusions.

The uppermost units of the Bayan Obo Group, the *Y14* to *Y17* and the *Y18* limestones (Fig. 2), are exposed in the northern part of the area covered by Fig. 3. The *Y14* to *Y17* unit is a thick-bedded micritic limestone of uniform gray color. The *Y18* unit is a coarsely crystalline white limestone that includes occasional gray beds. The white limestone was easy to identify on color-composite satellite images.

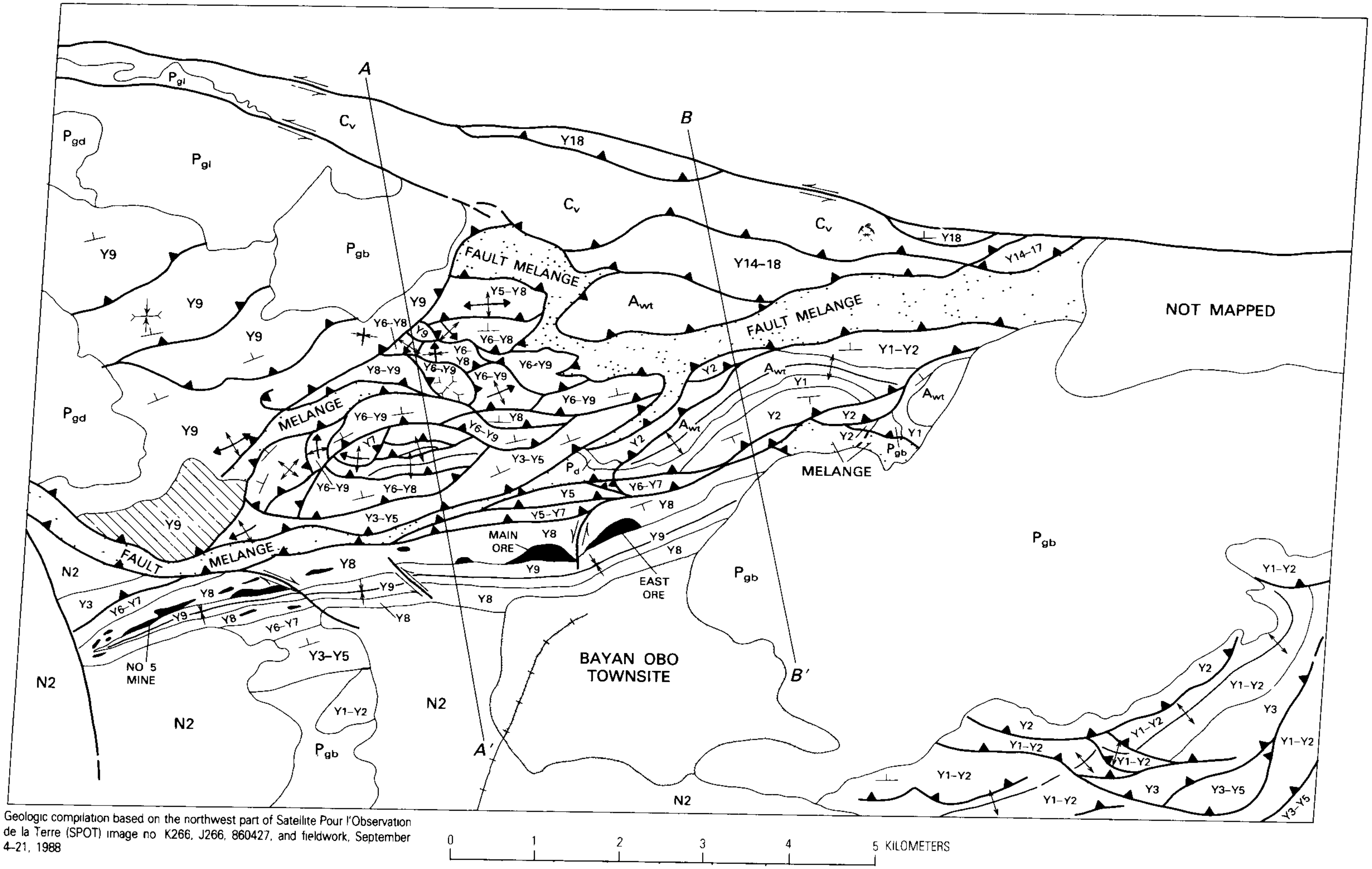

Geologic compilation based on the northwest part of Satellite Pour l'Observation de la Terre (SPOT) image no K266, J266, 860427, and fieldwork, September 4–21, 1988

Fig. 3. Geologic map of Bayan Obo area.

EXPLANATION

UNIT	DESCRIPTION	AGE
N2	Undivided sedimentary rocks	Tertiary Period
Unconformity. Age relations not implied		
P_d	Diorite	Permian Period
P_{gd}	Granodiorite	
P_{gb}	Biotite granite	
P_{gl}	Leucogranite	
C_v	Volcaniclastic and epiclastic rocks	Carbonaceous Period
Unconformity		

Combinations of rock units, within the Bayan Obo Group appear in the various fault blocks For example Y14–17 and Y18 as Y14–Y18

GROUP	UNIT	DESCRIPTION	AGE
Bayan Obo Group	Y18	White and gray limestone	Middle Proterozoic Era
	Y14–17	Gray limestone	
	Unconformity (?)		
	Y9	Black shale and intercalated carbonate rock	
	Y8	Limestone and dolomite and intercalated quartzite	
	Y7	Sandstone quartzite and limestone	
	Y6	Arkosic sandstone and quartzite	
	Y5	Thin-bedded carbonaceous shale	
	Y4	Dark quartzite	
	Y3	Carbonaceous shale	
	Y2	Tan to white quartzite	
	Y1	Coarse sandstone and basal conglomerate	
	Unconformity		
Wu Tai Group	A_{wt}	Migmatite	Archean Eon

- Hornfels
- Fault melange
- Volcanogenic massive-sulfide deposit
- Contact
- Fault, U, upthrown side, D downthrown side short dashed where uncertain
- Thrust fault, sawteeth on upper plate
- Tear fault
- Anticline showing crestline
- Dome
- Syncline, showing troughline
- Basin
- Strike and direction of dip of beds
- Mine

Explanation for Fig. 3.

A suite of volcanic rocks (C_v), which crops out in the Bayan Obo area (Fig. 3), is mapped as Carboniferous in age and occurs only in a thrust-fault-bounded tectonic slice. The rocks in this suite are subaqueous silicic volcanic and include rhyolite flows, domes, breccias, tuffs and epiclastic rocks and graywacke. During our 1988 season, we identified a Kuroko-type massive sulfide deposit within these volcanic rocks. This deposit is associated with the following upward-grading stratigraphy: rhyolite dome, vent facies, white exhalite that includes disseminated sphalerite, epiclastic rocks, graywacke and purple chert. A thrust fault terminates this stratigraphic section above the beds of purple chert.

The large volume of granitoid rocks of Permian age (Zhang and Tao, 1986) that crop out in the Bayan Obo area includes diorite (P_d), granodiorite (P_{gd}), biotite granite (P_{gb}) and leucogranite (P_{gl}). Numerous gold-bearing quartz veins and plugs, which are assumed to be associated with these granitoids, are found most frequently in the larger faults and fault melanges. Also serpentinite bodies crop out in the melange zone located in the west-central portion of the area shown in Fig. 3.

Structural geology

The structural geology in the Bayan Obo area is complex. During the Permian, a continent-to-continent collision severely deformed the passive margin on the northern edge of the north China plate (Wang Hongzhen, 1985). This deformation resulted in the formation of large folds, numerous thrust faults, duplex structures, basement horses and fault melanges. Each of these elements was mapped in the field; together, they exhibit a pattern consistent with thrust-faulted rocks found elsewhere in the world (King and Ferguson, 1960; Suppe, 1985). The tectonic transport during this collision was principally from northwest to southeast (Wang Hongzhen, 1985). The complexity of the thrusting in the Bayan Obo area is well illustrated by cross section *A–A′* shown in Fig. 4, which shows 13 emergent thrust faults; also shown are upright and overturned folds, domes, basins, and other interference structures; unfolded single- and multiple-bed segments; and basement horses. This disrupted package of rocks occurs as a roof pendant in the Permian granitoid rocks.

Cross section *B–B′* shown in Fig. 4 shows a large breached anticline that has a core of Wu Tai migmatite (A_{wt}) and a basement horse of Wu Tai migmatite above a zone of fault melange that is approximately 1 km wide. The large syncline at the southern ends of cross sections *A–A′* and *B–B′* contains the stratigraphic units that host the iron–rare-earth–niobium ore bodies.

Another element in the complexity of the structural geology of the Bayan Obo Group is the thrusting of younger over older rock units in the northwestern part of the map area (cross section *A–A′*, Fig. 4). This type of thrust-fault relation is caused by out-of-sequence thrusting, which is usually the result of two or more phases of deformation (Ramsay, 1967). Evidence for such polyphase deformation is evident in the basin-and-dome structures in the center of the study area and the curved fold axes, such as the fishhook termination, at the northern and of the large anticline in the southeasternmost part of the area (Fig. 3). The center of this anticline displays evidence for the development of a duplex structure that has tectonic transport toward the southwest. This provides further evidence that large-scale tectonic stress was applied in at least two directions – northwest–southeast and northeast–southwest.

Large-scale tectonic processes have also controlled the emplacement of serpentinites and the igneous rocks that crop out in the Bayan Obo area. The serpentinite bodies are located along the thrust fault (*Y9* fault melange zone) in the western central portion of the study area. These bodies are considered to be remnants of ocean crust that were emplaced in the fault zone during the Permian continent-to-continent collision.

The large volume of granitoid rocks of Permian age in the Bayan Obo area is also a result of this collision (Wang Hongzhen, 1985); these rocks apparently intruded along zones of weakness that were the previous locations of thrust faults. The granite body (P_{gb}) in the eastern part of the area shown in Fig. 3 and present within the Bayan Obo townsite and farther west conforms to the traces of the major thrust system north of the syncline that hosts the ore bodies. The outcrop pattern of this granite is also parallel to the principal direction of thrust-fault development in the southeastern part of the map area (Fig. 3). In addition, the three granitoid bodies in the northwestern part of the map area (Fig. 3) are

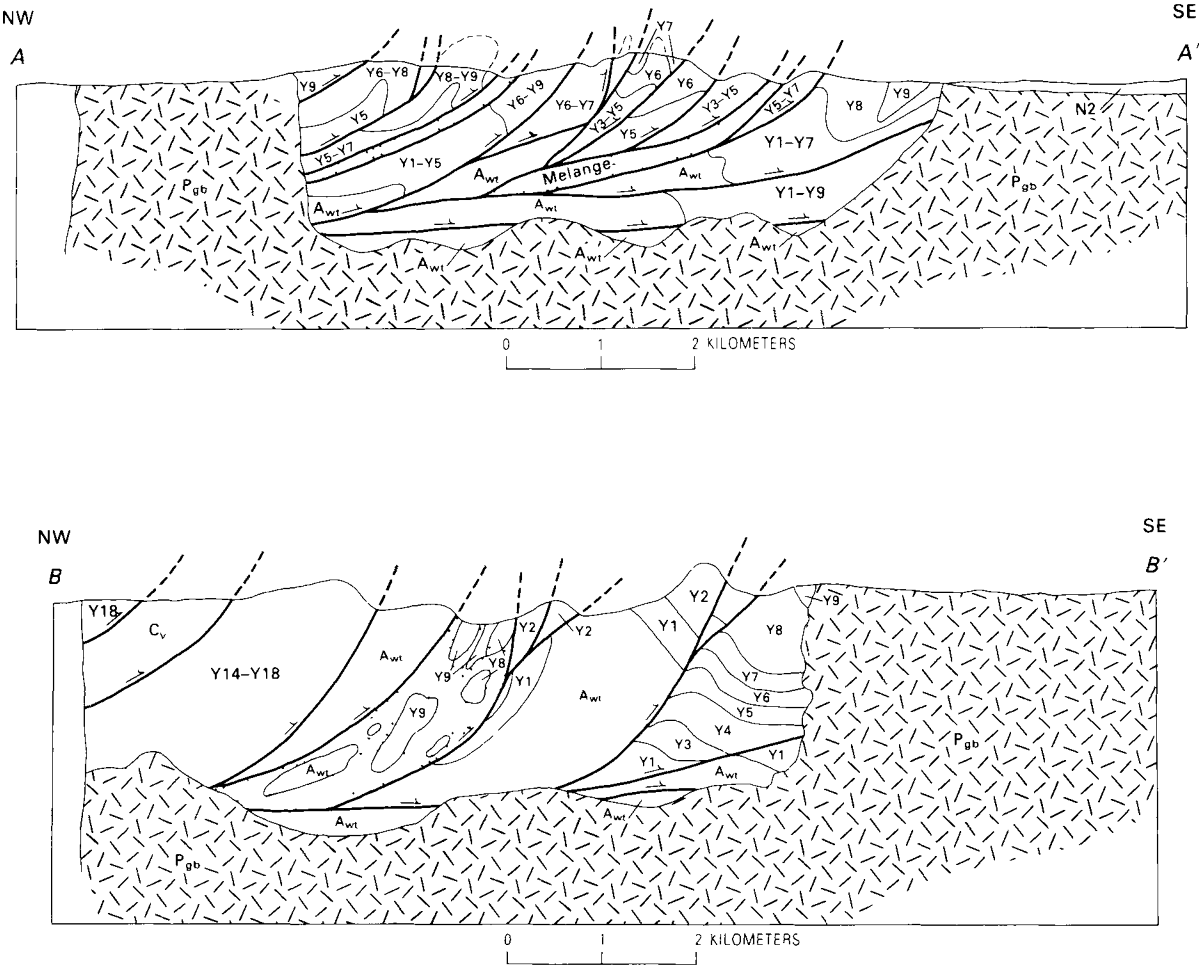

Fig. 4. Geologic cross sections *A–A′* and *B–B′* (see Fig. 3).

in the trace of the major thrust-fault melange zone that cuts across the north-central part of the area (Fig. 3). The leucogranite (P_{gl}) in this trend cuts the biotite granite (P_{gb}) and the granodiorite (P_{gd}) and has a highly evolved mineralogy that consists of potassic and sodic feldspar and quartz and sparse biotite as the only mafic mineral. Fluorite occurs widely in this leucogranite in veins and as irregular masses as much as several meters in length and width. Small bodies of diorite (P_d) crop out in a fault melange located in the very center of the map area (Fig. 3).

Hydrothermal alteration of host rocks

The hydrothermal system, which emplaced the ore bodies at Bayan Obo, created a large halo of wallrock alteration that is exposed over an area of about 50 km^2. This alteration includes mineralized selvages around the veins (and possibly dikes) and vein stockworks that cut the migmatites and clastic rocks in the footwall, as well as pervasive alteration of these rocks. The *Y9* shale in the hanging wall has also been intensely altered and brecciated. The spatial extent of these various types of wallrock alteration is shown in Fig. 5.

Footwall alteration

Large veins (possibly dikes) as much as 3 m wide that contain predominantly calcite cut the Wu Tai migmatite in the core of the breached anticline 1.5 km northeast of the East pit. The wallrock between these veins was altered by the introduction of iron,

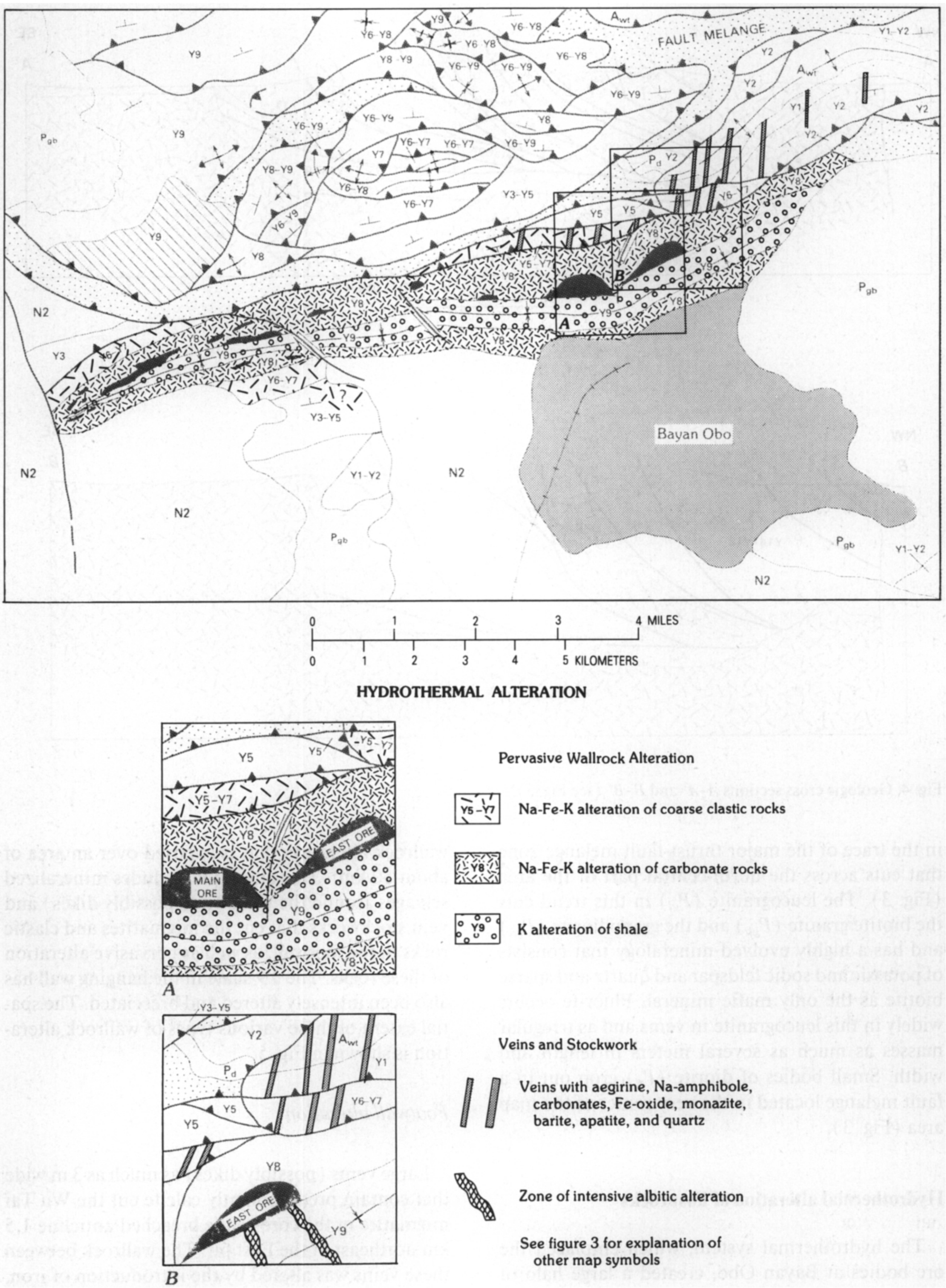

Fig. 5. Hydrothermal alteration map of Bayan Obo area.

sodium and potassium, thus producing a mineral assemblage dominated by aegirine, sodic amphibole, albite and potassium feldspar. Barite, magnetite, apatite and monazite are also common in the veins and the altered migmatitic wallrock.

A 1-m-thick vein that has a mineralogy dominated by aegirine and sodic amphiboles, which is similar to that in the altered zones, crops out together with smaller veins in the *Y1* sandstone and the *Y2* quartzite about 300 m south of the larger veins (possibly dikes) in the Wu Tai migmatite. Thinner veins of varying concentrations of the same sodic minerals occur on the southern flank of this breached anticline with decreasing frequency for nearly 4 km to the east of the location of the largest veins found in the Wu Tai migmatite.

Somewhat thinner veins, which range up to about 0.5 m in thickness and have approximately the same strike, crop out in the thrust-fault slice of *Y6* arkosic sandstone and *Y7* sandstone directly south of the breached anticline. This fault slice is also cut by many small veins (1–5 cm in width) and, in the center portion, these veins form a stockwork. The mineralogy of these veins is approximately the same as that of the larger veins that cut the Wu Tai migmatite and the *Y1* and the *Y2* units in the breached anticline directly to the north. With the exception of the purest orthoquartzite beds in the *Y2* unit, the wallrock around small and large veins is pervasively altered by the introduction of iron, sodium and potassium to form a mineral assemblage similar to that in the Wu Tai migmatite.

Another intensely developed stockwork of veins, which have individual thicknesses of 1/3 cm, is exposed in the fault slice containing *Y5* to *Y7* rocks directly north of the Main mine (Fig. 5). The mineralogy of these veins is again dominated by aegirine, sodic amphibole, magnetite, albite and barite. Lesser amounts of monazite, pyrite and carbonate minerals of various compositions also occur. Other minor minerals include an unusual oxide-mineral series that is composed of varying amounts of iron, titanium, niobium and zinc. Most of the coarser arkosic beds in this fault slice are so pervasively altered to sodic amphiboles that they are deep blue/green.

The *Y8* dolomite in the syncline that hosts the major ore bodies is pervasively altered in the same manner as the clastic rocks and the migmatites in the footwall. This alteration is clearly visible below the Main and the East ore bodies on color satellite images as a dark-brown halo. Most outcrops of the *Y8* unit have concentrations of sodic amphibole along bedding planes. Many of the thin beds of shale and silt in this unit are altered to sodic amphibole and mica, which ranges in composition from annite through biotite to phlogopite. Secondary iron oxide minerals, including various magnetite polymorphs and hematite, are present. These iron oxides occur in a continuum of sizes from individual grains disseminated throughout the host dolomite to larger masses as much as 20 cm thick, which are usually found along bedding planes, to concentrations of sufficient volume to be mined. These iron mines range in size from small, shallow, surface workings, where a few thousand tons of ore have been removed, to larger pits, where perhaps several hundred thousand tons have been mined, to the large-scale open pit operations at the Main and the East ore bodies, which are reported to produce more than 7 million tons of iron ore per year. The production of rare-earth oxides from these two mines in 1987 was reported to be about 15,000 tons of rare-earth metals.

The hydrothermal alterations of the *Y8* dolomite involved the introduction of a large amount of fluorine and the digestion of a similar volume of the host rock; for example, about 20% of the ore in the Main and the East ore bodies is composed of fluorite. The quantities of fluorite and iron ore together suggests that a large volume of dolomite was digested by the hydrothermal system and moved elsewhere. Also, much of the rare-earth ore is bastnaesite, whereas monazite is the only rare-earth ore mineral in the veins and the stockworks in the footwall rocks. Presumably, a large proportion of the rare-earth metals now occurring as bastnaesite was complexed with carbonate from the dolomite during deposition. Additionally, much of the magnesium that now occurs in phlogopite and the magnesium and the calcium that occur in the sodic and the nonsodic amphibole that replaced carbonate grains throughout the altered volume of the *Y8* dolomite are from hydrothermal digestion of the dolomite.

The partitioning of the rare-earth cations between the various phosphate and carbonate phases in the *Y8* unit is complex; for example, in some samples where monazite and apatite grains are found in contact with each other at the detection limits of the JEOL-840 scanning electron microscope (SEM), all the rare-earth cations have been precipitated in the monazite, whereas, in other samples, apatite grains very close (several hundred micrometers) to monazite grains show concentric cerium zoning.

Hanging wall alteration

The presence of the *Y9* shale above the *Y8* dolomite is thought to have contributed to the location and the concentration of the mineralization at Bayan Obo. The constituents of this shale reacted with the hydrothermal fluids to produce an impermeable caprock, which focused the chemical reactions that replaced *Y8* dolomite and resulted in the enormous concentration of iron, rare-earth metals and niobium at the top of the *Y8* dolomite and the bottom of the *Y9* shale.

At the outcrop and the hand-specimen scales, several aspects of the mineralogy of the *Y9* shale in the hanging wall are striking. First, along the entire strike length of the ore-bearing syncline, the mineralogy of the shale is essentially microcline feldspar. Second, two zones of nearly pure albite crop out in the hanging wall of the East ore body. The largest of these is about 20 m wide and the smaller zone is about 10 m wide. Third, the bottom portion of the *Y9* shale is brecciated, severely at some locations; at other locations, it is cut by several generations of small veins that locally developed into stockworks. A banding, which grades inward from potassium feldspar to biotite to fluorite, is common in the breccia matrix and veins. It is also common to find the matrices of the brecciated segments of the *Y9* shale to be dominantly potassium feldspar. The overall appearance of the *Y9* shale is flinty and has a conchoidal fracture. It is, for the most part, a very dark rock that has occasional wisplike white to gray patches. Brecciation is almost always present but may not be obvious in hand specimen. Curiously, the similarity is striking between the alteration of the *Y9* shale in the ore-bearing syncline at Bayan Obo and the metasomatic alteration (mineralogy and chemistry) and the brecciation of the Karroo mudstone around the Mwambuto Hills carbonatite in the Central African Rift System as described by Bailey (1960). The metasomatic alteration of the hanging wall *Y9* shale and that of the footwall rocks, which are discussed in some detail below, are based on the results obtained from the SEM, the optical microscope and the X-ray diffraction studies of 287 samples collected during the 1987 and the 1988 field seasons.

Petrographic, mineralogic and chemical analyses of selected samples

The fine-grained texture and widely varying compositions of the secondary minerals in the ores and the host rocks at Bayan Obo are most effectively studied by using the SEM. This instrument is particularly useful in determining the mineralogy and the replacement textures in the various metasomatites in the hydrothermal alteration halo around the deposits. It is equally useful for determining the mineralogy of the fine-grained material in the smaller veins and stockworks in the footwall rocks, as well as the coarser grained material that occurs in the veins that cut the Wu Tai migmatites and the overlying lower Bayan Obo Group sediments. Optical microscopy and X-ray diffraction were used in conjunction with the SEM to determine the mineralogy of many of these samples.

Carbonate veins and associated alteration in Wu Tai migmatite

The largest features associated with mineralization that crosscut the footwall rocks are a group of veins (as much as 3 m wide) in the Wu Tai migmatite that contain calcite and other carbonates of variable composition. The associated alteration in the wallrock is characterized by the assemblage of aegirine, sodic amphiboles, albite and potassium feldspar. Barite, apatite, Fe–Nb–Ti–Mn oxides and monazite commonly occur in the altered wallrock and, to a lesser degree, in the veins. The alteration halo between the veins and the altered wallrock is gradational; for example, individual aegirine, sodic-amphibole, albite and magnetite grains are surrounded by calcite near the edge of the vein (Fig. 6A), whereas, several centimeters into the wallrock, the mineral assemblage is characterized by sodic amphiboles, albite and potassium feldspar and lesser amounts of barite, Fe–Ti–Nb oxides and apatite (Fig. 6B). A sample taken from the central part of one of the largest carbonate veins contains calcite, magnetite, quartz, potassium feldspar, hyalo-

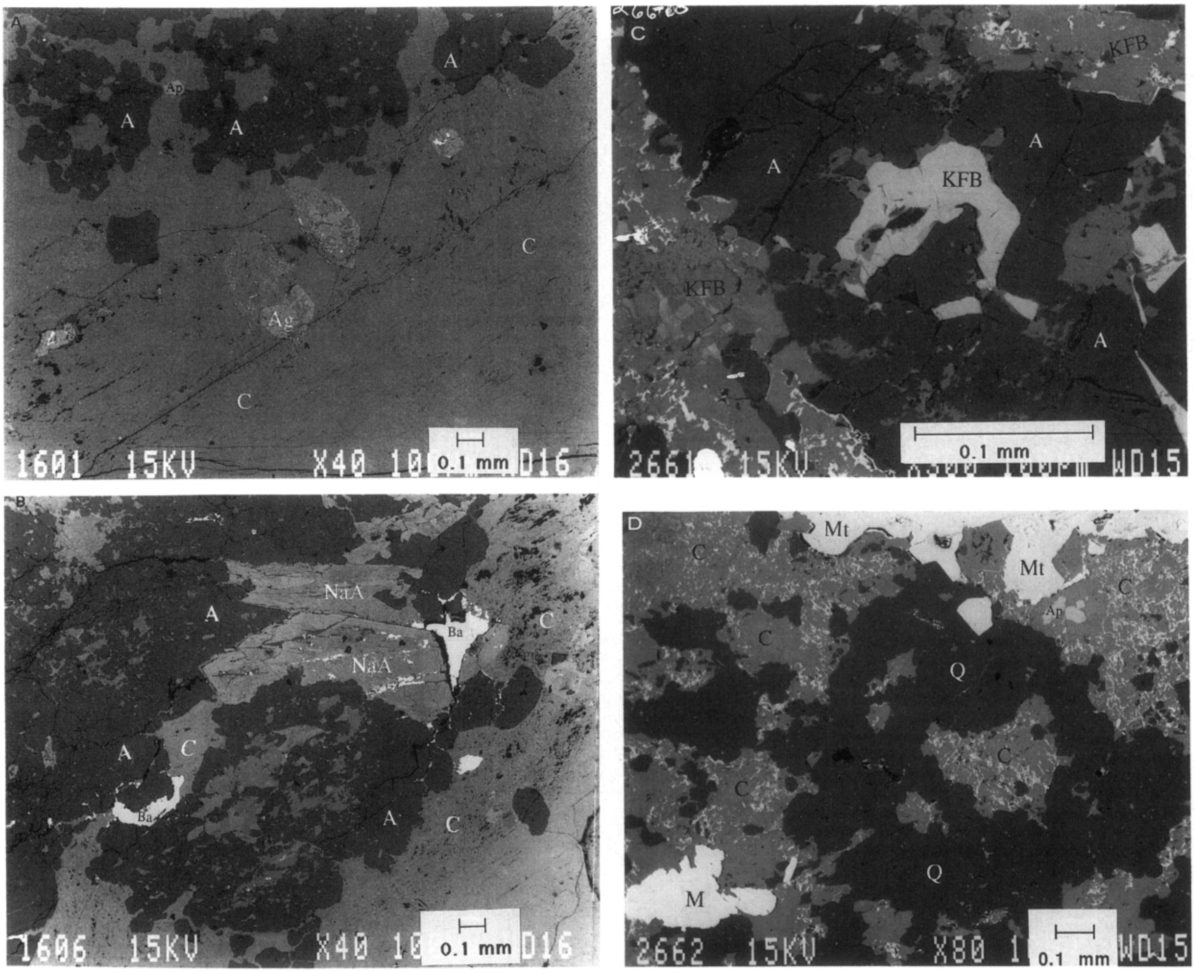

Fig. 6. Scanning electron microscope (SEM) photomicrographs of carbonate veins (dikes?) in migmatite of the Wu Tai Group (A) and (B), edge of 2-centimeter-wide vein; (C) and (D), center of 3-meter-wide vein *A*, albite; *Ap*, apatite; *Ag*, aegirine; *Ba*, barite; *C*, calcite; *KFB*, hyalophane; *M*, monazite; *Mt*, magnetite; *NaA*, sodic amphibole; *Q*, quartz.

phane (potassium-barium feldspar), albite, apatite and monazite (Fig. 6C, D). A Ti–Nb–Cr–Fe- oxide series mineral also occurs in this sample.

Veins cross-cutting the Y1 to Y7 footwall rocks and wallrock alteration

Irrespective of their width, the veins that cut the footwall rocks northeast of the East mine, the thrust fault slice directly to the south and a second thrust slice north of the Main mine contain aegirine and sodic amphiboles. Where these veins cut quartzite, the contact between the vein and the wallrock is sharp; sodic amphibole is the main mineral present in the veins, along with lesser apatite and monazite (Fig. 7A). In the interior of this vein, a 0.5-cm-wide zone of nearly pure aegirine occurs. Elsewhere in this vein, aegirine and sodic amphibole occur together with lesser quantities of barite, apatite, monazite, magnetite and quartz (Fig. 7b).

Although some of the orthoquartzite beds in the footwall are not altered, most beds have wide halos of secondary minerals next to the veins. In the coarser grained clastic rocks, particularly the arkosic beds in the *Y6* unit, sodic amphibole and xenoblasts of hyalophane are present (Fig. 8A). Some hyalophane xenoblasts contain relic albite. The replacement of albite by potassium feldspar and/or hyalophane is common in the footwall and the hanging wall rocks at Bayan Obo. Numerous mi-

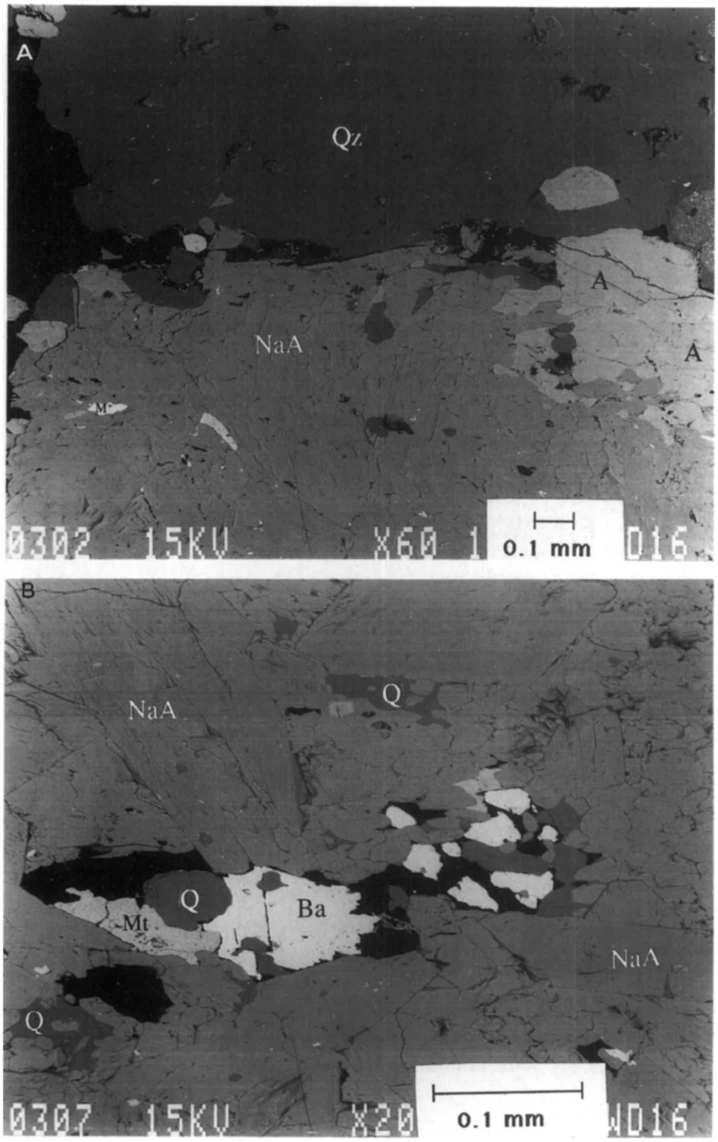

Fig. 7. SEM photomicrographs of 5-centimeter-wide vein crosscutting quartzite bed in arkosic sandstone (*Y6* unit). (A) edge of vein; (B) middle of vein *Qz*, quartzite; *A*, apatite; *NaA*, sodic amphibole; *M*, monazite; *Q*, quartz; *Ba*, barite; *Mt*, magnetite.

croveins occur throughout the coarser grained clastic rocks in the footwall and contain a diverse mineral assemblage of barite, monazite, apatite and magnetite and Ca–Fe–Mn–Sr–Zn carbonate series minerals (Fig. 8B).

A chemical analysis of the sample shown in Fig. 8B is given in Table 1 (sample *Y6b*). A companion analysis for a sample of *Y6* arkosic sandstone rich in potassium feldspar clasts, which is taken from a location 4 km north of the ore-bearing syncline, is also given in the Table (*Y6a*). The altered rock contains (as oxides) approximately 5 to 10 times as much iron, magnesium, calcium, sodium and phosphorus as the unaltered rock. The concentration of the rare-earth metals in the altered rock is also about five times greater than in the unaltered rock. The enrichment in these chemical constituents, along with the petrographic evidence seen in Fig. 8, shows the effect that hydrothermal solutions had upon the coarser grained rocks in the footwall. The relative concentrations of potassium and barium are reversed from what would be expected. This reversal

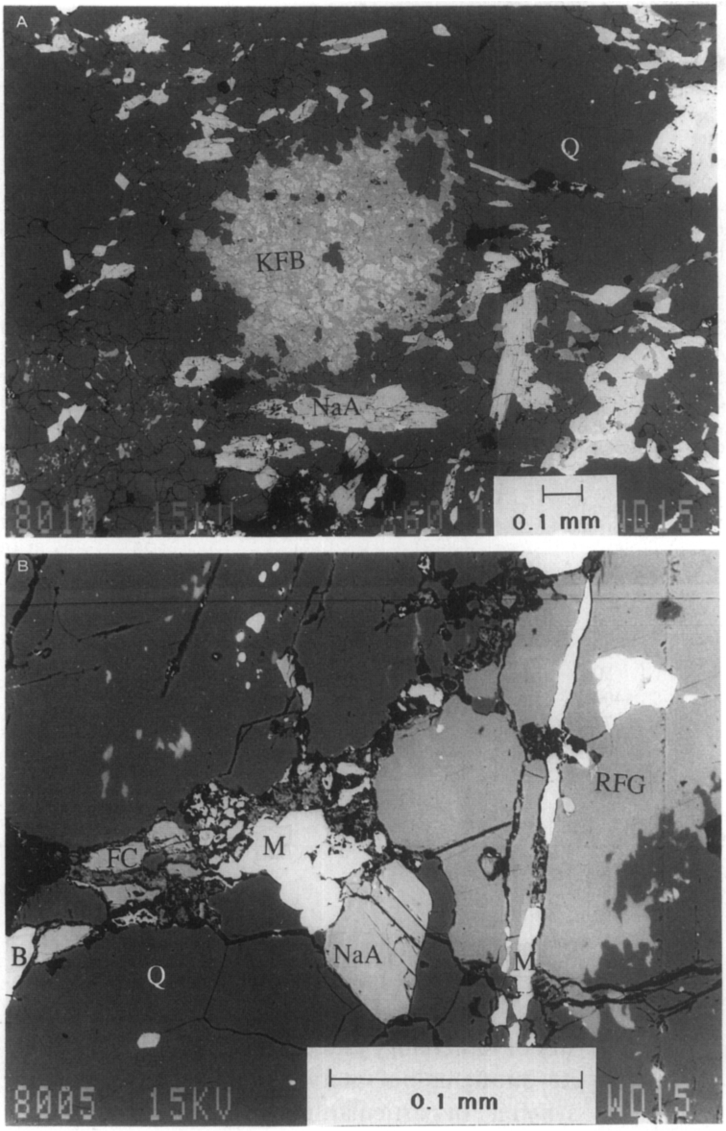

Fig. 8. SEM photomicrographs of two views (A) and (B) of fenitized arkosic sandstone (*Y6* unit). *KFB*, hyalophane xenoblast; *NaA*, sodic amphibole; *Q*, quartz; *RFG*, gneissic rock fragment; *M*, monazite; *B*, barite; *FC*, Fe-carbonate.

is attributed to the high concentration of potassium feldspar clasts in the unaltered sample. The altered sample is finer grained and most of the rock fragments are gneissic and richer in quartz than those in the unaltered sample.

Ore-grade samples from the Y8 dolomite

The ore in the *Y8* replacement bodies varies widely in composition within a single mine and across the mines. The major types of ore in the East and the Main mines are shown in Fig. 9. The ore bodies are zones and have iron-rich cores; the stratigraphically lower portions (north of the core) have a high fluorite content and the upper portions (south of the core) have a high sodic amphibole content (mapped as riebeckite). Aegirine occurs above and below the iron-rich core in the East ore body but only above the iron-rich core in the Main mine.

A SEM photomicrograph of a sample from the riebeckite zone near the top of the East ore body is shown in Fig. 10. This sample is approximately ore grade for iron (Table 1). It contains magnetite, fluorite, sodic amphibole and monazite. The rela-

TABLE 1

Chemical analysis of selected samples from Bayan Obo (LOI, loss on ignition)

Oxide or Element	Y6 Arkosic sandstone		Y8 ore East mine riebeckite zone	Y8 ore No. 5 mine	Y9 shale			
	unfenitized a	fenitized b			D23	D47	D72	D45
SiO_2	89.3	81.5	11 6	8.44	58.2	53.9	58.2	89.5
Al_2O_3	3.84	7 56	<0 14	0.43	12.8	16.7	16.9	4.68
Fe_2O_3*	0.35	2.56	33.9	68.2	9.65	5.62	5.6	1 72
MgO	0.12	1.27	5.32	3.38	3.8	2.84	1.99	0.46
CaO	0 09	0 40	18 3	5.02	0 62	0.52	0.19	0.05
Na_2O	<0.15	4.86	1.41	0.82	4.0	1.55	0.86	<0.15
K_2O	4.31	0.83	0.58	0.70	6.86	11.0	13.6	1.61
TiO_2	0.12	0.14	0.03	0.07	0.20	0.26	0.27	0.15
P_2O_5	<0.05	0.18	1.44	0.09	0.37	0.28	<0.05	<0.05
MnO	<0.02	0.06	4.91	5.62	0.26	0 12	0.07	<0.02
F	<0 01	0.04	10.2	0.25	0 43	0.15	0.25	0.01
H_2O+	0.23	0.29	0.15	2.60	na	0.66	0.65	0 96
H_2O-	0.05	0.05	0 12	0.20	na	<0.05	0.13	0.07
LOI	na	na	na	na	na	1.65	1.20	1.10
In parts per million								
Ba	1000	350	280	1000	8700	28000	5800	290
Nb	<20	20	1100	50	130	70	30	<20
Zn	19	42	990	1400	350	130	150	<4
La	5.6	29.0	10000	72	1100	210	18	15
Ce	10.0	45 0	25000	560	2100	330	30	24
Pr	1 1	5.4	na	na	na	na	na	2 9
Nd	4.7	20 0	11000	790	810	160	20	11.0
Sm	1.5	3 5	na	na	na	na	na	2.3

*Total iron as Fe_2O_3

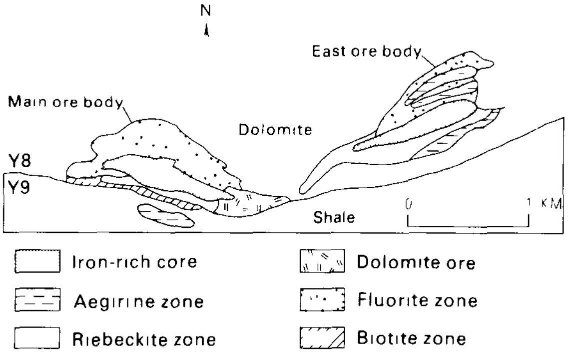

Fig. 9. Map showing major ore types in Main and East mines (modified from Bai and Yuan, 1985).

tively high concentration of manganese in this sample reflects high manganese concentrations of magnetite and sodic amphibole. A SEM photomicrograph of a sample from the top of the ore zone in the *Y8* stratigraphic unit at the No. 5 mine (Fig. 3) is shown in Fig. 11. The minerals in this sample include magnetite, Fe–Mn–Ca–Sr carbonate and sodic amphibole. The differences in mineralogy and chemistry between these two samples (Figs. 10, 11; Table 1) are typical of the diversity of mineralogy and chemistry in the *Y8* dolomite stratigraphic interval within the ore-bearing syncline. In particular, note the difference between the concentrations of the rare-earth metals and the fluorine (Table 1).

Sample from the hanging wall Y9 shale

The chemical composition, the mineralogy and the texture of the *Y9* shale in the core of the ore-bearing syncline yield additional information about the formation of the enormous volume of ore at Bayan Obo. Simply stated, the entire hanging wall in the ore-bearing syncline is a potassium metasomatite and potassium feldspar is the most common mineral. Biotite also occurs, particularly in the matrix of the ubiquitous breccias. Albite occurs throughout the hanging wall *Y9* shale as relic bodies of albitite. These bodies are interpreted as being un-

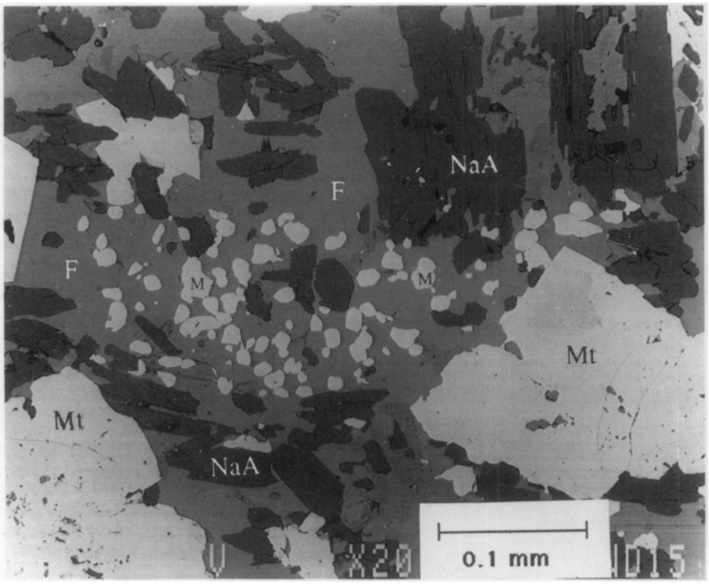

Fig. 10. SEM photomicrograph of riebeckite zone of East mine (in *Y8* unit). *F*, fluorite; *NaA*, sodic amphibole; *M*, monazite; *Mt*, magnetite.

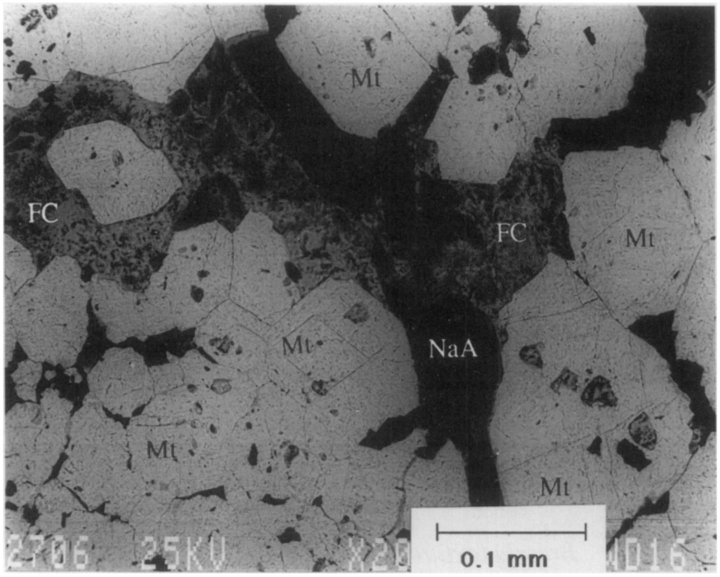

Fig. 11. SEM photomicrograph of ore sample from western ore body No. 5 (*Y8* unit). *Mt*, magnetite; *Fc*, Fe–Mn–Ca-carbonate; *NaA*, sodic amphibole.

digested remnants of an earlier, higher temperature phase of alteration from the hydrothermal system that emplaced the ore bodies. The largest of these relic bodies found to date is a steeply dipping, 20-m-wide zone of nearly pure albite that crops out in the East mine (Fig. 5). The smallest relics, which are only several micrometers wide, are the undigested remnants of individual albite grains (Fig. 12). The pattern of potassium feldspar replacing albite is associated with the cooling of the hydrothermal system (Hemley et al., 1980).

The formation of the potassium metasomatite in the hanging wall involved a complex sequence of deposition-solution-redeposition of mineral phases of varying compositions. Aspects of this sequence, where albite has been partly replaced by hyalo-

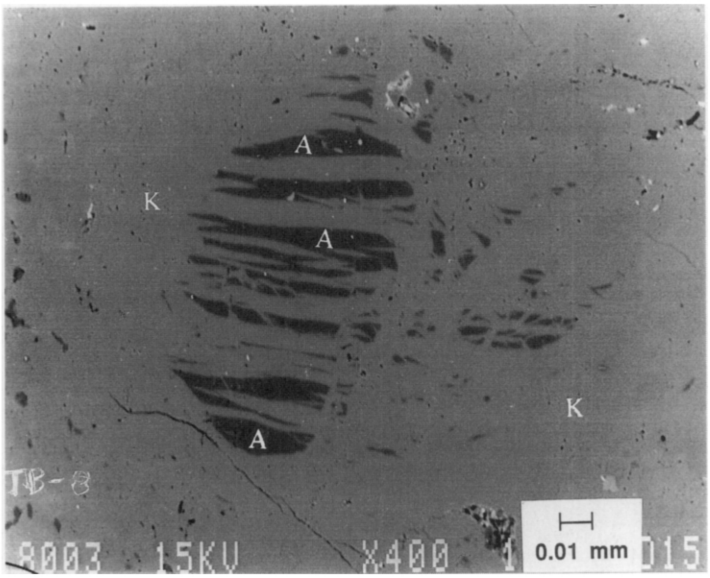

Fig. 12. SEM photomicrograph of K-metasomatite with relic albite grains (*Y9* shale unit, 40 meters above *Y8–Y9* contact in East mine). *K*, potassium feldspar; *A*, albite.

phane, are shown in the SEM photomicrograph in Fig. 13A. This replacement was followed by the partial replacement of the hyalophane and the previously unreplaced albite by potassium feldspar (Fig. 13B). Note the location of thin rings of hyalophane (about 1 μm in width) within several of the hyalophane grains. Some of these rings terminate at the grain boundaries, and others, completely within the grains; thus, solution and deposition of hyalophane was cyclic. The dissolution of hyalophane before deposition of potassium feldspar is most obvious in those grains where the barium-rich rings terminate at grain boundaries, showing that these grains have been embayed and/or are rounded. A chemical analysis from the facing slab of the thin section that was used to produce the photomicrographs in Fig. 13 is listed as D23 in Table 1. The barium content of this sample is nearly 1% (8700 ppm) and the sample also contains 6.86% K_2O and 4.0% Na_2O. Samples that contain 13 to 16% K_2O are common and are almost entirely composed of potassium feldspar. Presumably, these samples represent the complete replacement of all previous mineral phases by potassium feldspar, as suggested by the sequence of deposition displayed in Fig. 13. In many samples from the *Y9* stratigraphic interval in the ore-bearing syncline, this sequence of deposition stops with hyalophane as the last phase deposited in the metasomatite on a core of potassium feldspar (Fig. 14).

Apatite and monazite occur in nearly every sample of the *Y9* K-metasomatite collected. Apatite occurs as clots of grains and as individual grains (Fig. 15A). In Fig. 15A, a large (0.5 mm in length) grain of zoned hyalophane contains numerous inclusions of apatite. Clots of apatite grains also are present to the left of this hyalophane grain. Monazite appears in this sample as small, individual grains 2 to 10 μm wide and wormy, interstitial fillings 1 to 2 μm wide (Fig. 15B). In this sample, apatite grains are in contact with monazite and no detectable rare-earth metals are present in the apatite. In other samples, apatite is zoned in cerium content (Fig. 15C) and several other rare-earth metals.

Breccia textures

The pattern of brecciation in the *Y9* shale provides clear evidence that this shale served as the caprock that concentrated the hydrothermal fluids near the top of the underlying *Y9* dolomite in the ore-bearing syncline. This pattern of brecciation includes stockworks that are identical in appearance to those that were developed during the emplacement of the porphyry copper systems (Guilbert and Park, 1986). There, stockworks are composed of multiple sets of veins cutting each other at a variety

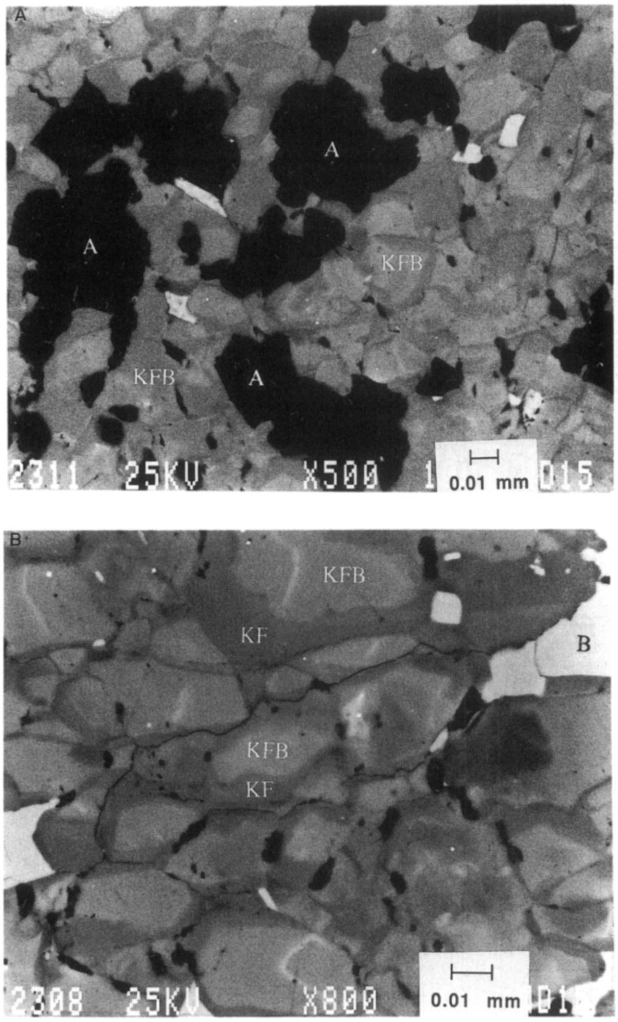

Fig. 13. SEM photomicrographs of replacement texture in sample D23 of *Y9* shale 85 meters above *Y8–Y9* contact at western mine No. 5. (A) hyalophane (*KFB*) replacing albite (*A*). (B) potassium feldspar (*KF*) replacing hyalophane (*KFB*).

of angles. This type of brecciation is well developed in the hanging wall of the East ore body at Bayan Obo. The breccia fragments consist of extremely fine grained potassium feldspar, most of which is opaque under the optical microscope. The veinlets in the stockwork are filled with a wide variety of minerals, including potassium feldspar, albite, biotite, fluorite, barite, monazite, bastnaesite, magnetite, pyrite and quartz. Another breccia texture that is frequently exposed in the hanging wall of the East mine is composed almost entirely of matrix material. This breccia is interpreted as being from zones in the hanging wall where large channelways developed in the shale.

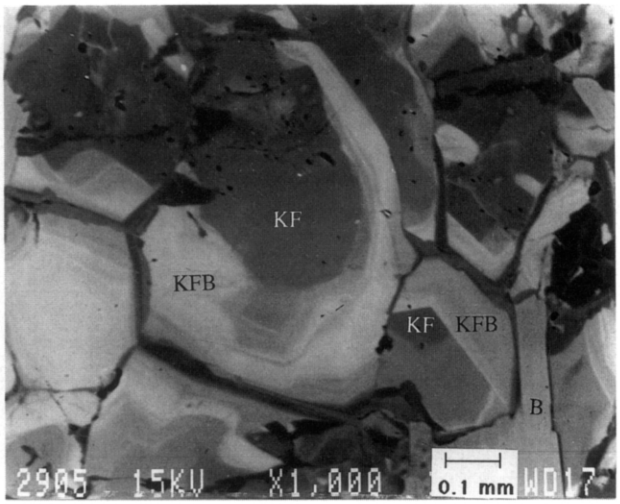

Fig. 14. SEM photomicrograph of K-metasomatite with hyalophane as last phase precipitated (*Y9* shale unit 41 meters above *Y8–Y9* contact at western mine No. 5). *KF*, potassium feldspar; *KFB*, hyalophane; *B*, biotite.

The most common breccia in the hanging wall is crackle breccia. This type of brecciation is developed throughout the *Y9* shale in the ore-bearing syncline. Although the bulk of the rock remained intact in this style of brecciation, bedding planes and other zones of weakness opened as the hydrothermal system dissipated its energy and fluids. In many of the samples, some rotation of the brecciated fragments occurred. The amount of matrix material in these crackle breccias usually is 5 to 10% of the total rock volume.

SEM photomicrographs of *Y9* shale crackle breccia located 62 m above the *Y8–Y9* contact in the East mine are shown in Fig. 16. The mineralogy of the crackle breccia fragments is dominated by potassium feldspar; minor albite and biotite also occur. The breccia matrix is composed of potassium feldspar, hyalophane and albite. This sample shows evidence for an inward filling sequence and a replacement sequence. The first mineral precipitated on the walls of the veinlets is fine-grained hyalophane mixed with albite (Fig. 16A). The texture of this albite shows that it has been partially reabsorbed and replaced by hyalophane. Elsewhere in this veinlet, albite was preferentially replaced by potassium feldspar along cleavage planes and microfractures (Fig. 16B). The interior of the veinlet shown in Fig. 16A is filled by biotite. Between the fine-grained hyalophane and albite precipitated at

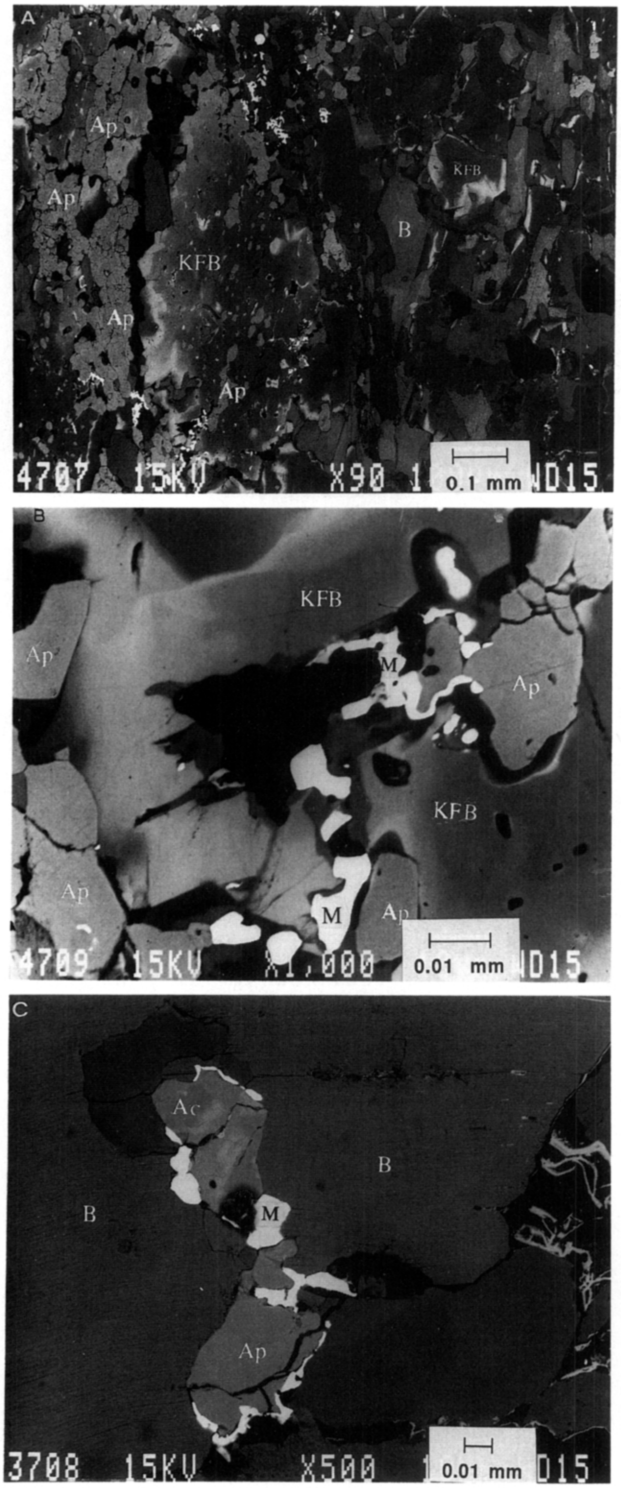

Fig. 15. SEM photomicrographs showing three views (A,B,C) of K-metasomatite containing apatite (unzoned and Ce-zoned) and monazite (*Y9* shale unit 46 meters above *Y8–Y9* contact at western mine No. 5). *Ap*, apatite; *Ac*, apatite Ce-zoned; *M*, monazite; *KFB*, hyalophane; *B*, biotite.

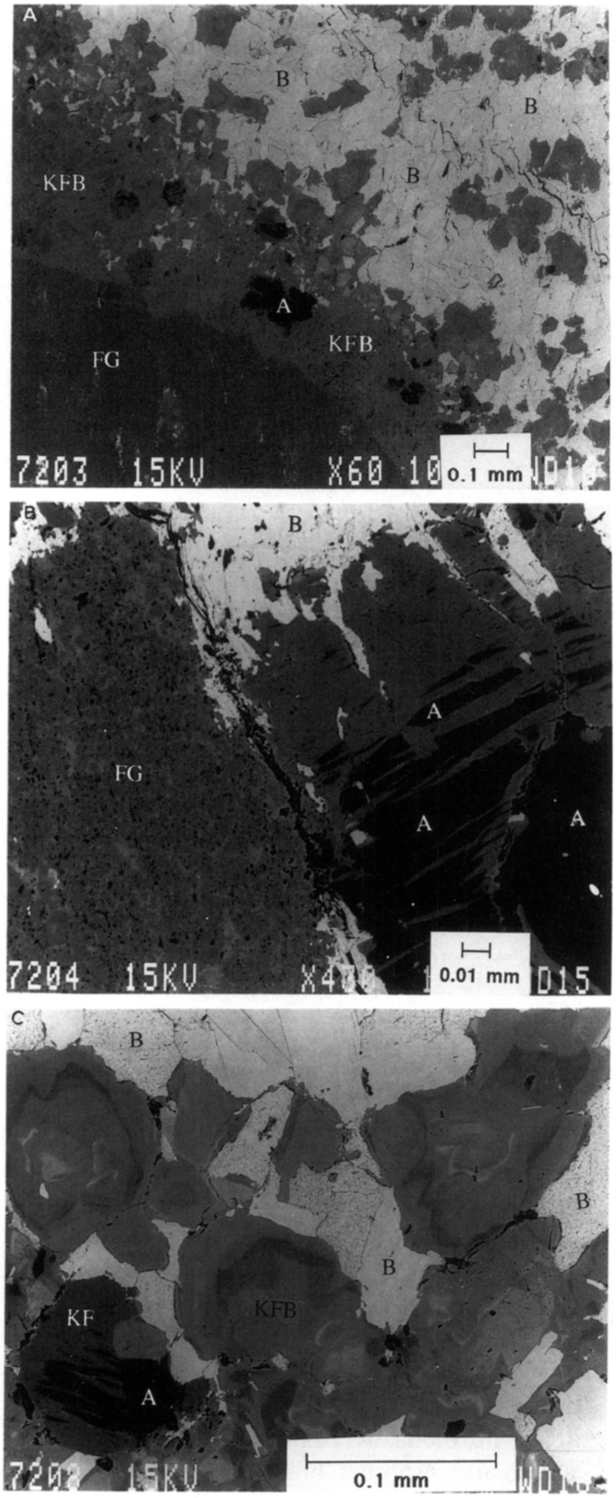

Fig. 16. SEM photomicrographs showing three views (A,B,C) of crackle breccia in *Y9* shale K-metasomatite, 62 meters above *Y8–Y9* contact in East mine. *FG*, breccia fragment (composed of potassium feldspar); *A*, albite; *KFB*, hyalophane; *B*, biotite; *KF*, potassium feldspar.

the wall of the veinlet and the biotite precipitated in the center of the veinlet, coarser grained hyalophane, which is strongly zoned with barium, was precipitated (Fig. 16C). The potassium feldspar that replaces albite has a composition similar to one of the interior growth rings in this hyalophane. Note that biotite has partially replaced the zoned hyalophane. Biotite is commonly the most stable mineral phase in the metasomatites at Bayan Obo.

The microcrystalline texture of the wallrock in the *Y9* potassium metasomatite, which is a breccia fragment, is shown in Fig. 16B. The mottled appearance is caused, in part, by the graphitic material that remained in the bulk of the metasomatite, presumably as the *Y9* shale was initially recrystallized by the hydrothermal system. The chemical analysis of the facing block from the thin section shown in Fig. 16 is given in Table 1 (sample D72). The bulk chemistry of this sample, which contains $K_2O = 13.6\%$, $SiO_2 = 58.1\%$ and $Al_2O_3 = 16.9\%$, is near the composition of potassium feldspar.

The overall pattern of hydrothermal alteration at Bayan Obo can be only partly reconstructed because structural disruption during the Permian deformation and subsequent erosion have removed much of the evidence; for example, the upward distal portion of the wallrock affected by the hydrothermal system is not present. All that remains of the top of the system is the *Y9* shale in the core of the ore-bearing syncline, which is an intensely altered proximal facies of the system. If some of the upward distal portion of the system had been preserved, then we could have traced the hydrothermal alteration of the *Y9* shale in the hanging wall from its incipient through its intermediate stages to its proximal alteration. A SEM photomicrograph of an unaltered sample taken from a thrust slice 4 km north of the Main mine is shown in Fig. 17. This sample of the shale is rich in quartz and has a silica content of 89.5% (Table 1, sample D45).

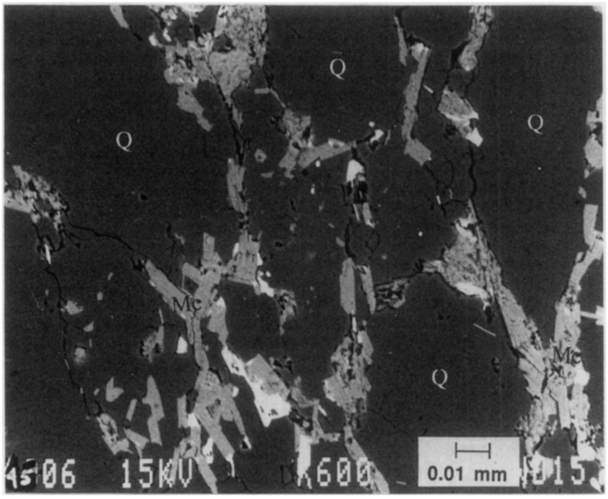

Fig. 17. SEM photomicrograph of unmineralized shale (*Y9* unit): sample is from thrust slice 4 kilometers north of Main mine. *Q*, quartz; *Mc*, muscovite.

Plate tectonic environment and possible age of mineralization

Bayan Obo is located on what was the rifted margin of the north China plate (Wang Hongzhen, 1985). The age of this rifting is estimated to have occurred in the interval 1850 to 1700 Ma (Wang Hongzhen, 1985). Ren et al. (1987) stated that the age of the Bayan Obo group is in the interval from 1650 to 1350 Ma. Isotope dating methods (Zhang and Tao, 1986) have yielded a range between 1800 and 1350 Ma for the age of deposition of the Bayan Obo Group. The Middle Proterozoic date of 1.400 Ma, which is based upon stromatolites, is commonly used as an age for the Bayan Obo Group (Hou Zonglin, Tianjin Geol. Acad., oral commun., June 1987).

An interpretation of the configuration of this rifted margin and associated aulacogens and microcontinental fragments is shown in Fig. 18 (Wang Hongzhen, 1985). Throughout much of the Middle Proterozoic, a large syndepositional fault was active along the rift margin (Fig. 18A, B). The cross sections in Fig. 18 (see Fig. 19 for location and explanation) illustrate the evolution of the northern continental margin, where more than 6000 m of sediment was deposited between 1400 and 1000 Ma. Isopach mapping in the vicinity of Bayan Obo has delineated several horst and graben structures that are filled with Bayan Obo Group sediments (Hou Zonglin, Tianjin Geol. Acad., oral commun., June 1987).

Radiometric dating problems

The age of the ore bodies at Bayan Obo is not known, but we speculate that their origin is associated with movement along the large fault system shown in Fig. 18. This is assumed to be a down-to-the-basin system initiated during rifting; continued

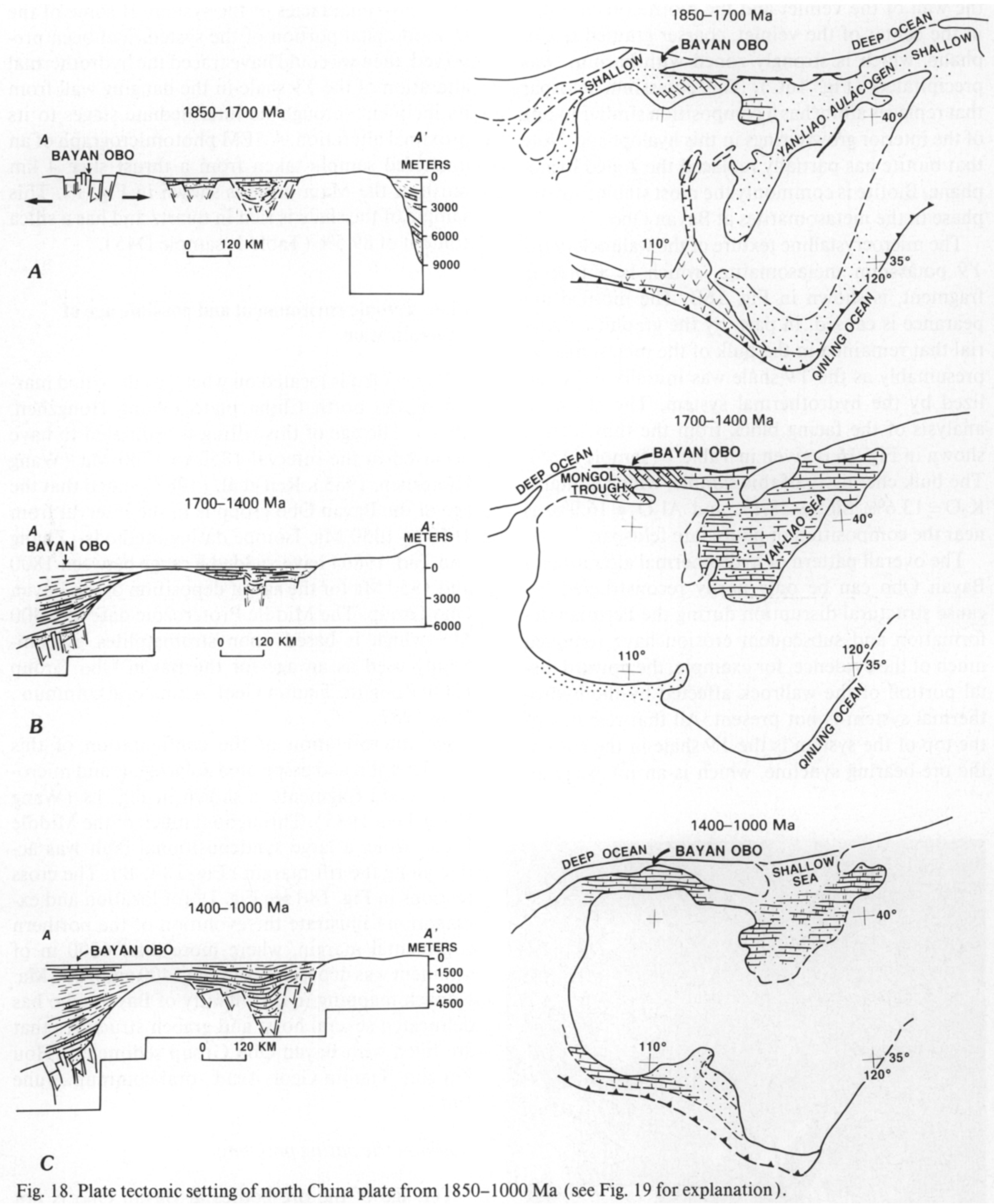

Fig. 18. Plate tectonic setting of north China plate from 1850–1000 Ma (see Fig. 19 for explanation).

movement occurred throughout the Middle Proterozoic and possibly later. Attempts to establish the timing of the many igneous events, including the mineralization at Bayan Obo, by isotopic methods have produced a wide range of dates (Tugarinov, 1963; Chao et al., 1989; Philpotts et al., 1989; Chao,

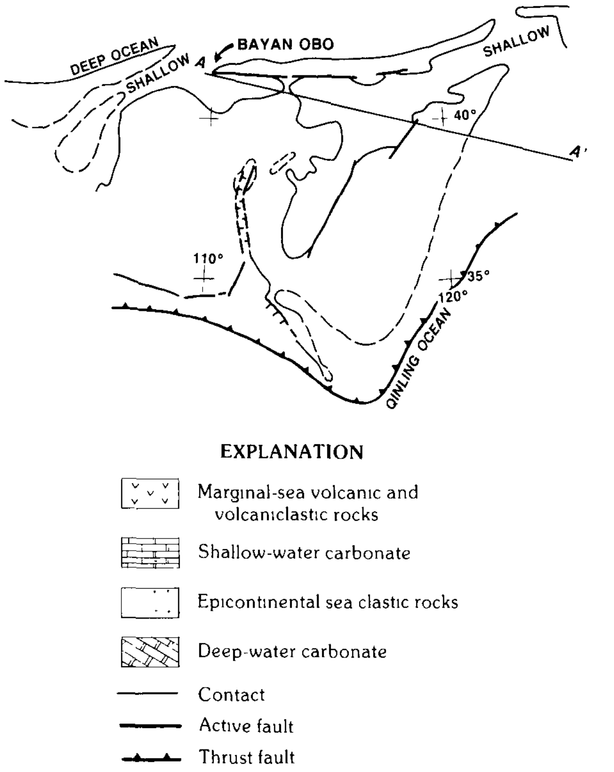

Fig. 19. Explanation for Fig. 18.

1990; E.D. McKee, U.S. Geol. Surv., oral commun., August 1989). These dates range from about 1400 Ma to about 240 Ma; groupings are between 650 and 850 Ma and 400 and 450 Ma and are based on Pb–Pb, Sm–Nd, Th–Pb, $^{40}Ar/^{39}Ar$ and K–Ar methods. The variable proximity of the samples dated to the enormous quantities of Permian granites (about 265 Ma; Chao et al., 1989) that surround and intrude the Wu Tai migmatite and the Bayan Obo Group (roof pendants) and that undoubtedly reheated and altered the isotopic system is probably one of the causes for the variable age determinations on samples from Bayan Obo.

Age of mineralization

The length and the duration of activity of the large syndepositional faults near Bayan Obo suggest that a deep-seated connection to mantle-derived material may have produced the hydrothermal fluids that form the ore bodies at Bayan Obo. Although mantle-derived intrusive rocks (the alkaline-carbonatite suite) do not crop out on a plutonic scale in the area around Bayan Obo, the large faults may have been the zones of weakness that allowed mantle material (gases and/or magmas) to rise high into the crust. In addition, we speculate that these faults also provided conduits for the hydrothermal fluids to escape from such magmas, to penetrate rocks of the Bayan Obo Group and to form the numerous iron–rare-earth–niobium deposits (Fig. 20).

The age of mineralization at Bayan Obo can be determined from field evidence to be pre-Permian; folding of the ore bodies unequivocally shows that they were emplaced before the northern margin of the north China plate was subjected to deformation during the Permian. Another clue to the possible timing of mineralization is the deposition of coarse-grained clastic rocks, including arkoses, during the Middle and the Late Proterozoic, as well as subaqueous volcanic rocks including massive sulfides, during the Carboniferous. On the basis of the sedimentation record, we can speculate that the cratonic margin in the vicinity of Bayan Obo was subjected to repeated rifting throughout the Proterozoic and possibly as late as the Carboniferous. Another element in this speculation is that the mineralization at Bayan Obo is very similar to that in ore bodies associated with carbonatite intrusions, which almost always are associated with incipient rift (hot spot) or rift environments (Sawkins, 1984).

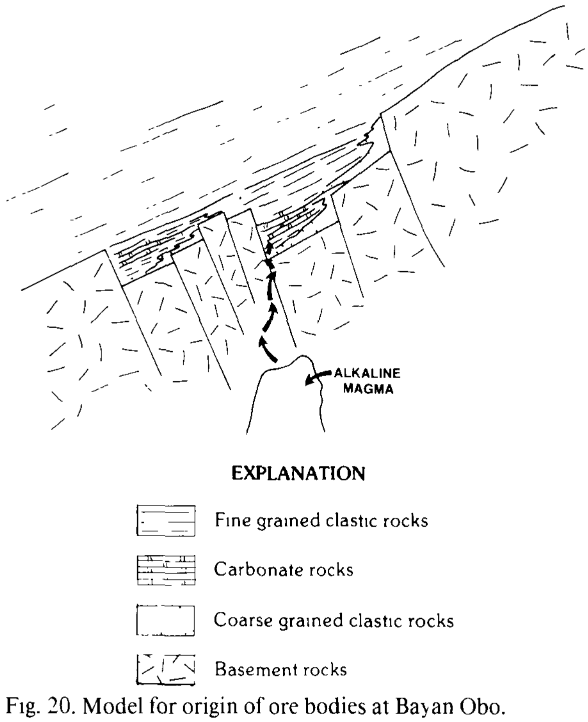

Fig. 20. Model for origin of ore bodies at Bayan Obo.

The tie between style of sedimentation and the rift setting offers a suggestion as to when the mineralization at Bayan Obo may have occurred. The earliest date that these ore bodies could have formed is shortly after the deposition of the *Y8* and the *Y9* units in the graben that developed on the edge of the craton; that is, a syn-rift timing of the mineralization during the Middle Proterozoic. Another possible time would be during the Late Proterozoic (Sinian Era, approximately 800 Ma), when a thick wedge of coarse-grained clastic material was deposited. These rocks crop out about 15 km southeast of Bayan Obo. By tying the deposition of this wedge of sediment to possible movement on the large fault system, which is on the edge of the craton, a Late Proterozoic age for the mineralization could be suggested.

Even though the subaqueous volcanic rocks of Carboniferous age that crop out near Bayan Obo are of considerable volume, they are probably not associated with the rifting event connected to the origin of the ore bodies. These rocks range in composition from andesites to rhyolites and the associated massive sulfide mineralization is of the Kuroko type, which suggests a subduction-related setting, such as a back-arc basin followed by accretion. It is also possible that these volcanic rocks could have formed in a minor rift basin on the edge of the craton. Until conclusive evidence is presented for the age of formation of the ore bodies at Bayan Obo, the possible connection to all pre-Permian rifting events with the origin of the ore bodies should be considered; for example, the Carboniferous volcanic rocks were deposited on the sea floor in a basin that could have formed on the cratonic margin associated with a fault system related to the large syn-rift fault system that was active on this margin of the craton during the Middle Proterozoic. Field work should be done to determine if these volcanic rocks were deposited in an island-arc environment and accreted onto the craton before the continent-to-continent collision during the Permian. If this can be established, then the rifting event that created these rocks can be removed from possible association with formation of the ore bodies at Bayan Obo.

Conclusions

The iron–rare-earth–niobium deposits at Bayan Obo, Inner Mongolia, China, are interpreted to have formed by hydrothermal replacement of the *Y8* dolomite unit of the Middle Proterozoic Bayan Obo Group. More than 20 ore bodies are located at or near the top of this dolomite. The *Y9* shale that overlies the *Y8* dolomite served as a caprock that contained the hydrothermal solutions in the dolomite. This shale was intensely brecciated and altered to a K-metasomatite by the same hydrothermal fluids that formed the ore bodies.

The footwall rocks are a series of sandstones, arkoses and shales that lie unconformably on a basement of Archean migmatites. These footwall rocks are cross-cut by a series of veins (possibly dikes) as much as 3 m in width. In several sections of the footwall, a vein stockwork was developed. A wide variety of minerals occur in these veins, including various Fe–Mn–Sr–Ca carbonates, various Fe–Ti–Nb–Cr oxides, barite, monazite, apatite, aegirine and sodic amphiboles. The wallrock near these veins was intensely altered by the introduction of iron, sodium and potassium.

The origin of the hydrothermal fluids that formed the ore bodies at Bayan Obo can be inferred from the plate tectonic setting of the host rocks and the resultant mineralogy of the ores. The host rocks are a sequence of syn-rift sediments deposited in a series of grabens that developed on the margin of the north China plate during Middle Proterozoic rifting. This tectonic setting of the host rocks, the mineralogy of the ore bodies and the associated alteration suggest that the hydrothermal fluids were derived from an alkaline-carbonatite intrusive series. However, with the exception of the large carbonate-bearing veins and/or dikes that crop out in the footwall, no plutonic rocks of alkaline or carbonatite composition have been identified in the vicinity of Bayan Obo. The extensive thrusting during Permian times may have separated these plutons from the current location of the ore bodies.

Acknowledgements

The authors wish to thank A.A. Drake, U.S. Geological Survey, Reston, Va., for his contribution to our understanding of the tectonics associated with the continent-to-continent collision during the Permian of the North China and Siberian plates. We also wish to thank Mr. Yang Zi Yuan for the contribution he made in the field and for his skill in oral and written language translation.

References

Bai, G. and Yuan, Z., 1985. Carbonatites and Related Mineral Resources. Bull. Inst. Miner. Deposits, 13, Geol. Publ. House, Beijing, 192 pp.

Bailey, D.K., 1960. Carbonatites of the Refunsa Valley, Feira, Northern Rhodesia. North. Rhod. Min. Labor Mines Bull. 5, 75 pp.

Chao, E.C.T., Minkin, J.A., Back, J.M., Okita, P.M., Mckee, E.D., Tosdal, R.M., Tatsumoto, M., Wang, J., Edwards, C.A., Ren, Y. and Sun, W., 1989. The H8 Dolomite Host Rock of the Bayan Obo Iron-Rare-Earth-Element Ore Deposit of Inner Mongolia, China-Origin, Episodic Mineralization, and Implications. U.S. Geol. Surv. Circ. 1035, p. 8.

Chao, E.C.T., 1990. Multiple Lines of Evidence for Establishing the Mineral Paragenetic Sequence of the Bayan Obo Rare Earth Ore Deposit of Inner Mongolia, China. IAGOD, August 1990, Ottawa.

Drew, L.J. and Meng, Q., 1990. Geologic Map of the Bayan Obo Area. U.S. Geol. Survey I-Map 2057.

Guilbert, J.M. and Park, C.F., 1986. The Geology of Ore Deposits. Freeman, New York, 985 pp.

Hemley, J.J., Montoya, J.W., Marinenko, J.W. and Luce, R.W., 1980. Equilibria in the System Al_2O_3-SiO_2-H_2 and Some General Implications for Alteration/Mineralization Processes, Econ. Geol., 75 (2): 210–228.

Hou Zonglin, 1987. Ore Genesis of the Bayan Ore Deposits of Inner Mongolia, China. Geol. Res. Acad., Min. Metall. Ind., pp. 1–10.

King, P.B. and Ferguson, H.W., 1960. Geology of Northeasternmost Tennessee. U.S. Geol. Surv. Prof. Pap. 311, 136 pp.

Meng, Q., 1982. The Genesis of the Host Rock Dolomite of Bayan Obo Iron Ore Deposits and the Analysis of its Sedimentary Environment. Geol. Rev., 28(5): 481–489 (in Chinese with English Abstract).

Philpotts, J.A., Tatsumoto, M., Wang, K. and Fan, P-F., 1989. Petrography, Chemistry, Age and Origin of the Rare-Earth Iron Deposit at Bayan Obo, China, and Implications of Proterozoic Iron Ores in Earth Evolution. U.S. Geol. Surv. Circ. 1035: 53.

Ramsay, J., 1967. Folding and Fracturing of Rocks. McGraw-Hill, New York, 568 pp.

Ren, J., Jiang, C., Zhang, Z. and Deyu, Q., 1987. Geotectonic Evolution of China. Springer, New York, 203 pp.

Sawkins, F.J., 1984. Mineral Deposits in Relation to Plate Tectonics. Springer, New York, 325 pp.

Suppe, J., 1985. Principles of Structural Geology. Prentice-Hall, Englewood Cliffs, New Jersey, 537 pp.

Tugarinov, A.I., 1963. Geochemical Features of Central Asian Metasomatites. In Geochemistry of Alkali Metasomatism. Acad. Sci. USSR Press, pp. 152–196 (in Russian).

Vlasov, K.A., 1968. Geochemistry and Mineralogy of Rare Elements and Genetic Types of Their Deposits. Genetic Types of Rare-Element Deposits, Vol. 3. Israel Program Sci. Transl. Ltd., 916 pp.

Wang Hongzhen, 1985. Atlas of the Paleogeography of China. Cartogr. Publ. House, Beijing, 143 pp.

Zhang, P. and Tao, K., 1986. Bayan Obo Mineralogy. Science Press, Beijing, 208 pp.

Zhou, Z., Li, G., Sung, T. and Liu, Y., 1980. Geologic Characteristics and origin of the Bayan Obo Dolomite Carbonatite of Inner Mongolia. Geol. Rev., 26: 35–41.